

Dalton Transactions

Accepted Manuscript



This is an *Accepted Manuscript*, which has been through the Royal Society of Chemistry peer review process and has been accepted for publication.

Accepted Manuscripts are published online shortly after acceptance, before technical editing, formatting and proof reading. Using this free service, authors can make their results available to the community, in citable form, before we publish the edited article. We will replace this *Accepted Manuscript* with the edited and formatted *Advance Article* as soon as it is available.

You can find more information about *Accepted Manuscripts* in the [Information for Authors](#).

Please note that technical editing may introduce minor changes to the text and/or graphics, which may alter content. The journal's standard [Terms & Conditions](#) and the [Ethical guidelines](#) still apply. In no event shall the Royal Society of Chemistry be held responsible for any errors or omissions in this *Accepted Manuscript* or any consequences arising from the use of any information it contains.

ARTICLE

CPMV induced synthesis of Hollow-porous SiO₂ Nanocapsules with excellent performance in Drug delivery

Cite this: DOI: 10.1039/x0xx00000x

Koushi Kumar^a and Pradip Paik^{*a},

Received 00th January 2012,
Accepted 00th January 2012

DOI: 10.1039/x0xx00000x

www.rsc.org/

An idiosyncratic hollow mesoporous-SiO₂ nanocapsule has been synthesized at room temperature using unmodified Cowpea mosaic Virus (CPMV) as a template, and without using any catalyst or surfactant during synthesis. The average size of the capsules synthesized is ~200-250 nm with 60-100 nm hollow core these nanocapsules have been characterized through high resolution transmission electron microscopy (HRTEM). Biocompatibility of the hollow mesoporous SiO₂ nanocapsules has been investigated with MTT assay using the RAW 264.7 cells, HepG2 cells (human liver carcinoma cells) and Hek293 cells (human embryonic kidney cells). Nanocapsules are loaded with fluorescent molecules (rhodamine 6G), doxorubicin (DOX) an anticancer drug and chloroquine diphosphate (CQDP) an antimalarial drug and their release have been studied through UV-Vis spectrometer. Development of surfactant free, bio-safe, hollow and mesoporous SiO₂ nanocapsules with CPMV has provided a route of synthesis of porous nanocapsules towards drug loading and sustained delivery of drugs. The synthesis method of hollow porous SiO₂ nanocapsules using CPMV is novel, straight forward and further demonstrating the generality of the nano-formulated capsules that can be used for various drug deliveries based therapeutic applications. To check the *in vitro* efficacy in medical biotechnology, Hek293 and HepG2 cell lines are used and studied the cell viability of DOX loaded hollow silica nanocapsules. Results show that our bio SiO₂ nanocapsules synthesized with CPMV is an effective cargo and suitable in nanoformulating with DOX and the resultant nanoformulation is very promising in killing cancer specific cells.

Introduction

Hollow nano-particles or nano-capsules^[1,2] are emerging as one of the most promising tools in medical biotechnology for a variety of therapeutic applications such as target drug delivery for treating cancer or tumour cells,^[3-8] gene delivery and molecular bio-imaging.^[9-11] Till date, an enormous determination have been devoted to explore a suitable material and method to accomplish hollow nanocapsules based on polymers,^[3,5,6] liposomes,^[12] inorganic metals^[13-15] and oxides,^[4] with specific surface properties, as it becomes very important for the therapeutic applications otherwise the drug loaded capsules fall off the target tissues due to cell turnover.^[16,17] Selective etching based on structural difference has also been employed to produce hollow inorganic and mesoporous core shell nanocapsules.^[18-19] Reported hollow nanocapsules have been synthesized in various approaches *e.g.*, template synthesis^[6] using nanoparticles (*e.g.*, Ag, Au, SiO₂, ZnO), self-assembly process^[20-21] *etc.* Most of these

approaches are restricted by the compositions, size, and surface properties so as to administrate medicine to the target site and by the biocompatibility of the capsules. The limitations of using nanocapsules in delivery of medicines are dwelling to the low loading efficiency and sluggish mass transfer to the target sites.^[22-24] Although the use of hollow nanocapsules advances to protect the drugs or genes, still they are very unstable in physiological environments, and they are readily excreted via kidney, non-specifically absorbed through the reticuloendothelial system and they delay/destroy/alter the standard cell activities and thus creating side effects.^[16-17,25] A number of research works on the synthesis of hollow organic or inorganic SiO₂ have been reported using different types of surfactants, where organic and inorganic nanocapsules are synthesised with control over size and shell thickness. There are extensive and vast research works in nanotechnology dedicated toward the biological/bio-medical applications. Where various organic and inorganic materials have been contributed to this field out of which silica based materials show a major share and

recently they have been extensively studied in various fields of medical applications.^[26] Changing the morphology such as from hollow SiO₂ nanospheres to nanotubes are demonstrated with the change in precursor and surfactant concentration.^[27-28] However, functionalized amorphous SiO₂ are attractive towards improvising the performances of drug delivery due to its good biocompatibility. But, most of the reported hollow SiO₂/other nanocapsules are synthesized using surfactants in highly basic medium (e.g., sol-gel, Stöber method^[29]) or with sacrificial template^[30-33] which are not easy to extract from the solid network structure and requires high temperature calcination. Further, it is a challenging task to reduce the toxicity due to the presence of entrapped unwanted residue of templates and surfactants. Therefore, producing porous hollow nanocapsules using a natural bio-template such as plant virus have a new era in producing functional nanocapsules for therapeutic applications such as for drug delivery. Nanocarriers are aimed to improve the performance as drug-carriers, in making them more biocompatible, water-soluble, reduced toxicity and high differential uptake efficiencies. A number of various plant virus are reported as bio templates to synthesize solid core-shell nanostructure materials and mainly they are chemically modified Cowpea mosaic virus (CPMV),^[34] positive standard Brome mosaic virus (BMV),^[35] cylindrical Tobacco mosaic viruses (TMV), a positive-sense single stranded RNA virus,^[36] Cowpea chlorotic mosaic viruses (CCMV),^[37] etc.. Viral nanoparticles have their own limitations in fabrication of nanostructured materials due to their shape, size, and surface functional groups present. Genetically modified CPMV has been used as template to synthesise solid core-shell metal nanoparticles (Pt, Au, Ag, Co etc.) and bimetallic nanoparticles.^[38] Similarly, genetically modified CPMV (chimaeric) are used with specific peptides sequence to deposit SiO₂ to get solid core-shell nano particles using silicate precursor^[39] and metallic particles from metal salt precursors. TMV virus particle can only give the virus-SiO₂/inorganic core shell nanoparticles with high aspect ratio due to its cylindrical shape.^[40-43] A study has been carried on synthesizing TMV-Ni core-shell nanoparticles through electroless deposition of Pd-Ni-Si (layer-by-layer deposition) on the genetically modified TMV as anodic material in Li ion battery application.^[44]

Herein this work, we report on the synthesis of a porous and hollow SiO₂ nanocapsules using CPMV which is a plant virus. This virus is used as a template without modifying its surface chemical structure and without using any surfactant. And finally we have studied the drug delivery efficiencies of hollow SiO₂ nanocapsules and cytotoxicity of hollow SiO₂ nanocapsules. Advantages of using CPMV particles are, (i) it is 28-30 nm in diameter with icosahedral symmetry, (ii) contain 60 copies each of a large and small coat proteins which actually interact with the silicates to deposit on it and helps to create the shell and (iii) show stability over a wide range of pH and at room temperatures at least for 24 hr and stable at 4°C in PBS (pH~4-9) at least for six months,^[34,45-50] which make it malleable towards the synthesis of hollow SiO₂ nanocapsules without using any surfactant or catalyst at room temperature.

Development of surfactant free, bio-safe, hollow and porous SiO₂ nanocapsules with CPMV has provided an enhanced efficiency towards drug loading and suitability for sustained delivery. A clear mechanism for the formation of hollow mesoporous SiO₂ nanocapsules has been demonstrated. The detailed physical and surface chemical properties of the hollow mesoporous SiO₂ nanocapsules have been studied systematically. A few number of reports have concentrated on the mechanistic manipulation of the micro structure design, properties and stability study during the fabrication process of hollow mesoporous SiO₂ nanocapsules using genetically or chemically unmodified CPMV. Further, these hollow mesoporous SiO₂ nanocapsules are explored for loading and release studies of fluorescent dye (Rh6G), antimalarial drug (CQDP) and anticancer drug (DOX). Finally two basic types of cell lines vis-a-vis noncancerous and cancerous have been used and studied the cell viability with and without the nanoformulation of anticancer drug (DOX) *in vitro* using RAW 264.7 cells (murine leukemia virus transformed), Hek293 cells (Human embryonic kidney cells) and HepG2 cells (Human carcinoma cells), respectively through biochemical MTT assay and investigated the efficacy of our nanoformulation for clearing the cancer cells is also investigated.

EXPERIMENTAL SECTION

All the chemicals were purchased from commercial suppliers and used without further purification. Tetraethylorthosilicate (TEOS, 98%), (3-Aminopropyl) triethoxysilane (APTES, 98%), Rhodamine 6G (Rh6G, 95%) and Chloroquine diphosphate (CQDP, 98%) and Doxorubicin Hydrochloride (DOX, 98%) were purchased from Sigma Aldrich. Sodium phosphate dibasic (99%), sodium phosphate monobasic (99%), sodium hydroxide (97%), Polyethylene glycol-6000 (PEG-6000, 98%), Sodium chloride (NaCl, 99%) were purchased from SRL chemicals.

Isolation of CPMV. CPMV infected leaves were thoroughly washed with Milli-Q water, then weighed and homogenised with 0.1 M PBS (pH~7.2) with a ratio of 2 mL/g of infected leaves. The homogenised leaves were passed through cheese cloth to collect the extract. Then, the extract was purified from the residue of leaves by centrifugation (at 10000 rpm (9,300 g) for 15 min). Then polyethylene glycol (PEG, M_w: 6000) was added into the solution to make a final concentration of 4% of the solution followed by the addition of NaCl to give a final concentration of 0.2 M. Then the mixture was stirred at 25°C to get a homogeneous solution. After 1-2 h the precipitate was collected by centrifugation (at 17000 rpm, 15,500 g, for 15 min). Then the precipitate was resuspended in 0.01 M PBS (pH~7.2). Finally the virus particles were purified by ultracentrifugation (at 40,000rpm, 1,37,000 g for 2.5 h) and preserved it in a freezer for further use (at -4°C).

Synthesis of hollow silica nanocapsules. A mixture of TEOS and APTES (90 and 10 mol percentage of silica sources) 72.5

μL volume was added to a 1.5 mL of aqueous solution containing CPMV (in PBS, pH ~ 7.2). The mixture was thoroughly stirred and left stationary for 72 h. After 72 h the reaction mixture was kept in water bath at 40°C for 24 h. With time the formation of white precipitate was observed after addition of silica source. Control sample was prepared from a mixture of TEOS and APTES with the same ratio (90 and 10 mol percentage) in PBS in the absence of CPMV keeping all other experimental condition same. A series of samples were also prepared by varying molar ratios of TEOS and APTES (e.g., 95:05 and 80:20) maintaining reaction conditions same, with keeping fixed CPMV volume to verify the role of precursor mixture. The reaction mixtures become white within 3-4 h for the mixture with 5 mol percent of APTES, for APTES of 10 mol percent it took 1.5-2 h and immediate precipitate formation was observed for 20 mole percent of APTES. Finally, all the samples were washed with PBS to remove the impurities and unreacted substrates.

Loading of Rh6G, CQDP and DOX. The thoroughly washed hollow SiO_2 nanocapsules were collected and dried for 24 h in vacuum. The fixed amount (1000 μg) of hollow nanocapsules (three sets) were incubated separately in Rh6G, CQDP and DOX solution with a concentration of dye/drug to hollow SiO_2 nanocapsules ratio of 1:1 mg/ml in PBS. The suspensions were vortexed separately for 1 h and then kept it for 24 h without further stirring.

Study of Rh6G, CQDP and DOX release kinetics using UV-Vis Spectroscopy. The suspensions of hollow SiO_2 nanocapsules-Rh6G and hollow SiO_2 nanocapsules-CQDP and hollow SiO_2 nanocapsules-DOX were subjected to centrifugation (at 10000 rpm, 9,240 g) for about 10 min) and the supernatant was removed leaving behind the loaded particles. These loaded particles were washed for few times with PBS to wash out the free drugs/dye from the surface of the capsules. After washing the loaded particles were air dried, resuspended it into PBS (pH ~ 7.2) at $\sim 37^\circ\text{C}$ for release studies. The samples were kept in a water bath maintaining the temperature at 37°C throughout the entire period of the experiment. And with fixed time interval absorbance of the release medium was recorded and the experiments were performed at 37°C . These measuring processes were carried out until there was no change in the absorbance due to the release of the dye or drugs.

MTT assay. *In vitro* cytotoxicity of mesoporous hollow SiO_2 nanocapsules was measured using MTT assay against RAW 264.7 cells (murine leukemia virus transformed), HepG2 cells (Human carcinoma cells) and Hek293 cells (Human embryonic kidney cells). Further *In vitro* cytotoxicity assay of DOX loaded hollow SiO_2 nanocapsules were carried out on HepG2 and Hek293 cell lines according to our previously reported method.^[51] In brief, 3-(4,5-dimethylthiazol-2-yl)-2,5-diphenyl-tetrazolium bromide (MTT) assay was performed in 96 well culture plates using growing RAW 264.7, HepG2 and Hek293

cell lines. 100 μL of medium containing $\sim 5 \times 10^3$ cells was taken in each well of 96 well plate and the plate was incubated in CO_2 incubator with 5% CO_2 injection at 37°C for 24 hrs. Next day the various concentrations of hollow SiO_2 nanocapsules and DOX loaded hollow nanocapsules were added to each well to get final concentration ranging from 0 to 100 $\mu\text{g}/\text{mL}$, respectively. Three sets were prepared for each concentration to minimize the error. 100 μL of untreated cells in medium was used as control. Then the cells were incubated in CO_2 incubator (5%) for 24 h at 37°C . After 24 h incubation 20 μL of 5 mg/mL MTT prepared in 1 x PBS was added to each well in dark and incubated in CO_2 incubator for 3 h. Then 50 μL of PBS was added to each well and incubated for 5 min and then the absorbance was recorded at 570 nm with microplate reader (BioTek, SYNERGY H4 HYBRID MULTI-DETECTION MICROPLATE READER, USA). Cell viability at each concentration was calculated using the eq: viability (%) = $(\text{ABST} / \text{ABSC}) \times 100$.

Where the ABST and ABSC are the absorbance of treated and control cultures, respectively at 570 nm.

Characterizations. The scanning electron microscopic (SEM) studies were carried out using a HITACHI S-3400 N scanning electron microscope. The aqueous samples were sonicated for 15 min, and then a few drops were taken on a glass slide followed by drying. The dried drop casted slides were sputter coated with Au-Pd. Then SEM images were taken using 15kV as AC accelerating voltage. The elemental compositions were confirmed by the EDS attached with the instrument.

The transmission electron microscopy (TEM) images and selected area electron diffraction (SAED) were obtained using a high resolution transmission electron microscopy (HRTEM) (FEI TECNAI G2). Preparation of HRTEM sample for CPMV: Stock solution containing CPMV was diluted by adding 0.1 of stock into 1 ml of 0.01 M PBS and drop casted on C coated Cu grids (200 Mesh). A drop of stain (2% of phosphotungstic acid) is added to the grid and kept for 10 seconds. Then the excess of the stain was wicked and rinsing was performed gently with excess Milli-Q water. A thin aqueous film on the surface of the grid was formed and it was dried in vacuum at RT. These negatively stained grids were used for TEM experiments to study the size and morphology of CPMV with an accelerating voltage between 120-160 kV. TEM sample preparation of hollow SiO_2 nanocapsules: 0.5-1.0 mg of hollow SiO_2 nanocapsules were dispersed in aqueous solution (1 mL water) and sonicated for 10 min, then a drop of the dispersed sample was taken on the C coated Cu grids and dried in vacuum for overnight and subsequently performed the HRTEM experiment with an accelerated voltage of 200 kV and SAED pattern was acquired for the same to study the crystal structure. N_2 adsorption-desorption experiments was performed at 76.5 K with a ASAP 2020 physisorption analyzer (Micromeritics Instrument Corporation), based on the adsorption branches of N_2 sorption isotherms; the Brunauer-Emmett-Teller (BET)

method was used to calculate the surface area of the porous and hollow SiO_2 nanocapsules.

The solid state crystal structure of the samples were characterized by an X-ray Diffractometer (X Bruker D8 Advance) using $\text{Cu K}\alpha$ ($\lambda = 1.5406 \text{ \AA}$) radiation operating at 40 kV/30 mA with a 0.02 step size and within the 2θ range of 10–90°.

IR-active vibration characteristics were recorded using Fourier transform Infrared spectroscopy (FTIR) with Nicolet, model: Impact-410. The dried samples was mixed with KBr in the ratio of 1:5 in pestle and mortar, and then pressed into disks and the spectra were recorded in the range of 4000–400 cm^{-1} .

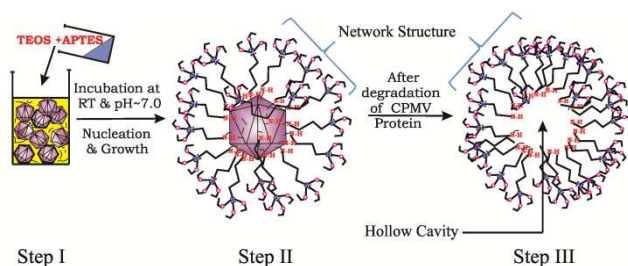
The UV-Vis absorption spectra for all samples were recorded using a UV-Vis-NIR spectrometer (Perkin Elmer: LAMBDA 750). The release of the dye and drug from the loaded hollow SiO_2 nanocapsules were studied in PBS (pH~7.2) at 37°C. At a certain interval of time the aliquot of release medium was taken out and UV-Vis-NIR spectra were recorded until there was no change in the intensity of the spectra. This process was repeated for three times for each batch of the sample.

Atomic Force Microscopy INTEGRA Aura model (NT-MDT, Russia) was used to investigate the surface topography and non-contact mode was used for scanning. CPMV stock solution was diluted and drops casted on to mica sheets and surface was scanned for surface topography.

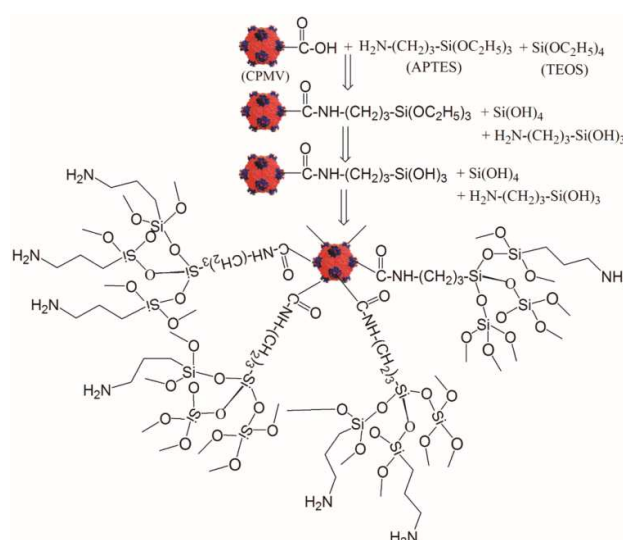
Dynamic light scattering (DLS) was performed using MS3000 model (Malvern Instruments Ltd., UK) to find out the distribution of particle size, where water was used as a dispersant medium for all the sample.

Results and Discussion

The results obtained here represent as a proof-of-concept for hollow and porous structure of SiO_2 with unmodified CPMV.^[36] Metals/oxides (Co , Fe_3O_4)^[52] are synthesised with chemically modified CPMV and structures with equivalent size of virus have been shown, but here the aim to develop hollow structures/capsules, which can be used for the nanomedical applications. According to our approach, where chemically or genetically unmodified CPMV are taken and about which a network of silicate is formed in presence of (3-aminopropyl) triethoxysilane (APTES) and tetraethyl-orthosilicate (TEOS)



Schematic I: Proposed synthesis mechanism in three steps (Step I, Step II and Step III).



Schematic II: Reaction steps involved in the process of making hollow nanocapsules

(Step I and II of Scheme 1) due to the electrostatic interactions between carboxyl/carbonyl or amine groups of CPMV and NH_2 groups of silicates. Then the protein residues of CPMV are denatured in PBS (pH~7.2) at elevated temperature and diffuses out from the core followed by the creation of hollow cavity (Step III, of Schematic I). The reaction scheme has been shown in Schematic II.

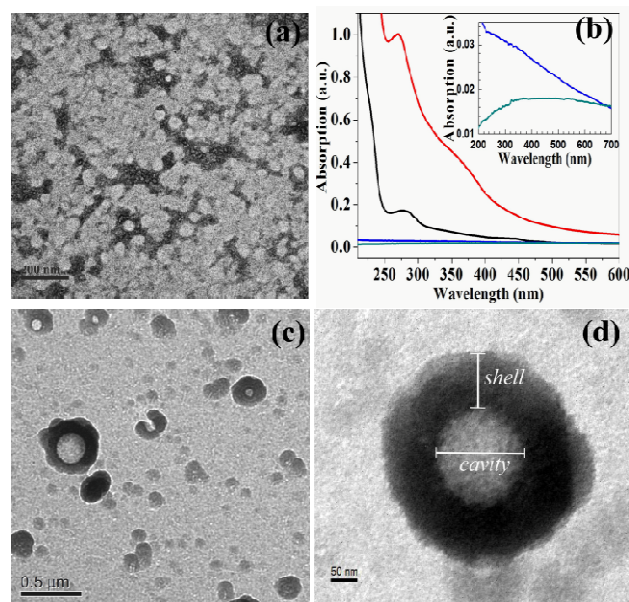


Figure 1: (a) TEM of CPMV, (b) UV-Vis absorption spectra (crude CPMV (red), purified CPMV (black), SiO_2 synthesized without CPMV (blue) and hollow SiO_2 after removal of CPMV (black)) in-set of (b) enlarged view of SiO_2 synthesized without CPMV (blue) and SiO_2 nanocapsules after removal of CPMV (purple), (c) TEM of SiO_2 nanocapsules and (d) HRTEM of a single SiO_2 nanocapsules.

The silicate formation followed the steps as it is mentioned in schematic II: first a bioconjugate is formed with the amide bonds (-CO-NH-), between -COOH of CPMV and -NH₂ of APTES and in the later stage it gets hydrolysed along with TEOS and/or APTES followed by the condensation and nucleation. The average particles size of CPMV is found to be ca. ~28-30 nm in diameter (Figure 1a) and the absorption peak is observed at 260-280 nm (Figure 1b) is due to the presence of protein in the icosahedral structure, and these results are matching well with the literature.^[48] Control sample was prepared by adding mixture of silane source (TEOS and APTES) to PBS without CPMV particles and keeping all the other experimental conditions fixed (See ESI: Figure 1S).

A series of reactions were carried out with various molar ratios of TEOS: APTES and in presence of purified CPMV (See ESI: Figure 2S) in PBS keeping all the other experimental conditions same. We observed that the different molar ratios of TEOS: APTES have the potential to affect a number of reaction parameters, including the rate of hydrolysis of the ethoxysilane groups, the overall degree of silica condensation, and interactions between the amine groups of the silica framework and the protein of CPMV which reduces the formation of core size as well as SiO₂ shell of the hollow nanocapsules. The purified CPMV only can give us SiO₂ nanocapsules with uniform size, shape and hollow core (Figure 2c). The size of the hollow SiO₂ nanocapsules are ca. ~200-250 nm in diameter with a shell thickness of 60-65 nm when the pure CPMV was used. Nanocapsules are segregated by centrifugation depending on their size. DLS studies of segregated hollow SiO₂ nanocapsules revealed the hydrodynamic diameter of the nanocapsules to be ~195 nm (See ESI: Figure 3S (a) and Table S1 (a)) and hydrodynamic diameter of hollow SiO₂ nanocapsules without subjecting it to centrifugation was found to have ~335nm. (See ESI: Figure 3S(b) and Table S1(b)). This segregates that the fused particles are obtained since we have not used any surfactant during synthesis. However, once the ratio TEOS: APTES increases to 1:1, the thickness of the shell increases, size and shape becomes non uniform since the formation of the silica nucleates on CPMV templates become uncontrolled (See ESI: Figure 4S). Bulk surface morphology of the nanocapsules is investigated from the SEM and interestingly found that these hollow nanocapsules are self-assembled to form a bigger micron sized hollow structure. This self-assembly can be possible due to the van der Waals forces of attraction or due to the other electrostatic interactions such as hydrogen bonding, intermolecular interactions *etc.* acting between the hollow nanocapsules to achieve its lowest free energy state (Figure 2a, 2b). The formation of hollow cavity larger than the diameter of CPMV (~30 nm) at the center of the nanocapsules can be attributed to the formation of aggregates/coagulates of many CPMV particles caused by the interparticle hydrogen bonding or aggregation of adjacent silica nucleates formed on the surface of the viruses during growth process.

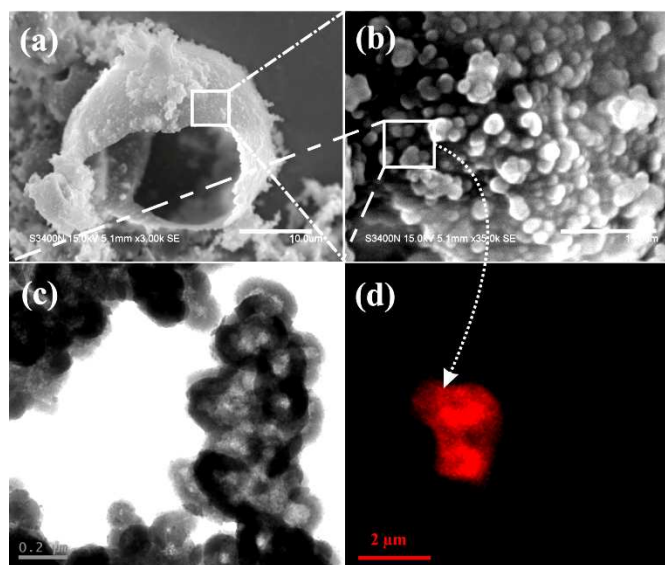


Figure 2. (a) SEM image of a single hollow capsules formed through self-assembly of hollow SiO₂ nanocapsules synthesized in presence of CPMV, (b) surface textures of the same formed by the self-assembly of nanoparticles (Scale bar 10.0 μm and 1.0 μm respectively), (c) TEM of hollow SiO₂ nanocapsules (shown in (b)) and (d) Confocal microscopy image of hollow SiO₂ nanocapsules loaded with Rh6G.

From Figure 2c, it is evident that the denatured CPVM particles from the centre of the particles create a defined hollow cavity at the centre of the nanocapsules. This excretion occurred in PBS (pH~7.2) at 40°C and it occurred due to the denaturation of amino acids of CPMV, when the products were cured at 40°C for 24 hrs and therefore subsequently CPMV losing their native structure. To check the stability of CPMV, similar experiment with CPMV was carried out (without SiO₂) and found that it did not show any UV-Vis absorption due to the protein at λ_{\max} ~ 260-280 nm, confirming proteins have lost their integrity. Other possibility of creation of micro porous structure is due to the formation of network of silicates. The porosity of the shell of the nanocapsules has been confirmed by loading of small fluorescence molecules such as Rh6G (Figure 2d). After denaturation the debris of CPMV after excreted through micropores (size below 2 nm) and mesopores (average dia. 5-10 nm) on shell which have been complimentarily confirmed through HRTEM (Figure 3) as well as with the BET N₂ gas adsorption-desorption measurements.

The BET surface area (Figure 4(a)) is found to be 78.6±0.45 m²/g (Langmuir surface area = 124± 0.35 m²/g) at P/Po = 0.276, with BJH desorption (Figure 4(b)) average pore diameter ca. 5-10 nm, and pore volume ca. 0.45 cm³/g at P/Po = 0.990, respectively. The particle size of the nanocapsules is also calculated from the BET experiment and found to be ca. 76.3 nm which is matching well with the results obtained from the HRTEM. The average size of the micro pores is found to be ca. 1.7 nm in diameter (from BET).

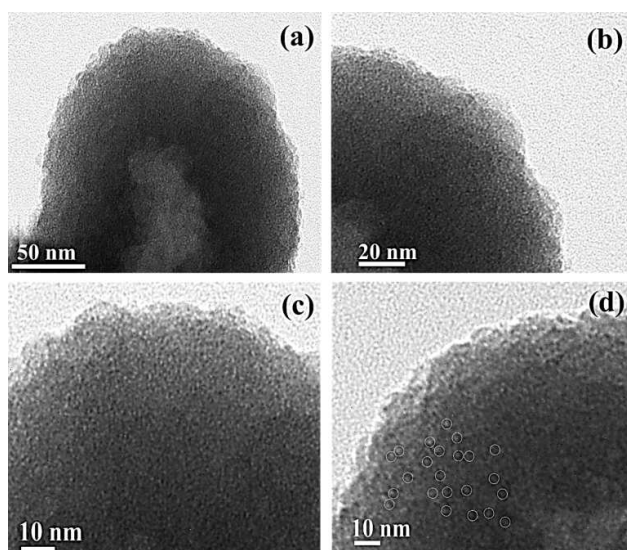


Figure 3. HRTEM Images of CPMV Hollow SiO₂ nanoparticles (lower and higher magnifications), (a) scale bar at 50 nm, (b) scale bar at 20 nm, (c) scale bar at 10 nm and (d) scale bar at 10 nm (with white spots on the particles highlighting the micro-pores on the shell of nanocapsules).

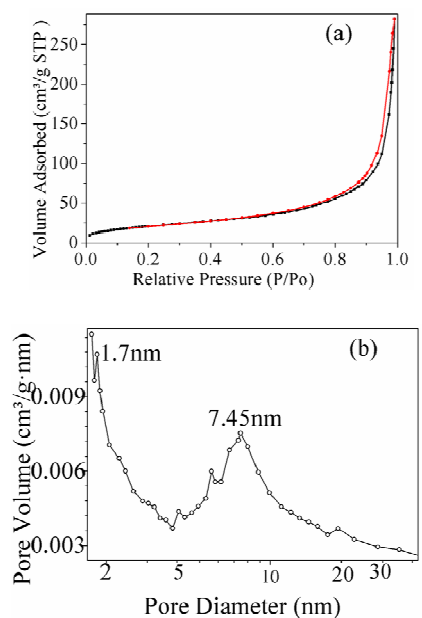


Figure 4: (a) BET adsorption (black) and desorption (red) isotherm of hollow SiO₂ nanocapsules, (b) pore size distribution of hollow porous nanocapsules, calculated from desorption isotherm.

Additionally, the surface chemical structure of the hollow SiO₂ nanocapsules has been investigated through FTIR spectroscopy analysis, and depicted that the capsules are functionalized with -NH₂ and -OH (Figure 5). The asymmetric stretching of Si-O-Si at 1080 cm⁻¹, asymmetric vibration at Si-OH at 943 cm⁻¹ and symmetric vibration at Si-O-Si at 795 cm⁻¹, characteristic vibration band at 3440 cm⁻¹ assign to the

stretching vibration of O-H presence in Si(OH)_x or -N-H but not from the O-H of water as the experiments were carried out in N₂ atmosphere and the samples were thoroughly dried. The absorption peak appeared at 1640 cm⁻¹ is due to the -N-H deformation vibration.^[53-54] TEOS and APTES are taken as silicate sources, where APTES is an aminosilane from which the 1640 cm⁻¹ vibration arises, this vibration can also be seen from the sample which was synthesised in absence of CPMV.

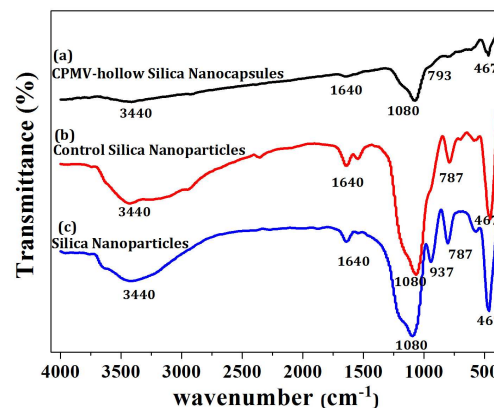


Figure 5: FT-IR Spectra of (a) Hollow SiO₂ nanocapsules prepared in presence of CPMV (b) SiO₂ synthesized without CPMV in PBS, (c) SiO₂ synthesized with NH₃OH in absence of CPMV.

These functional groups advances the self-assembly process to form hollow capsules. Both the powder XRD (see ESI: Figure 5S) and SAED pattern obtained from TEM confirms the predominantly amorphous nature of hollow SiO₂ nanocapsules (see ESI: Figure 6S). Novel porous hollow SiO₂ nanocapsules exhibited biocompatibility which has been initially confirmed through the MTT assay using the RAW 264.7 cell lines at 37°C (Figure 6). The different concentrations of the sample were taken (e.g., 10, 25, 50, and 100 µg/ml). The results revealed that more than 90% cells remained alive after 24hr of incubation at the maximum concentration of nanocapsules. Therefore, novel SiO₂ nanocapsules having a unique structure which can be used for medical biotechnology such as for drug and gene delivery applications. To promote the usefulness of this material for delivery applications a series of cell based studies have been performed under living body conditions.

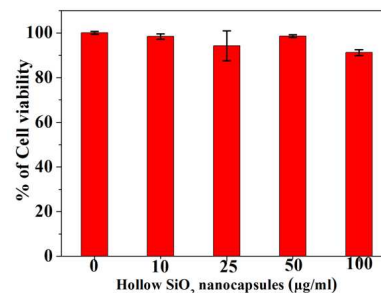


Figure 6: Cell viability measured by MTT assay in RAW 264.7 for mesoporous hollow SiO₂ nanocapsules synthesized with CPMV.

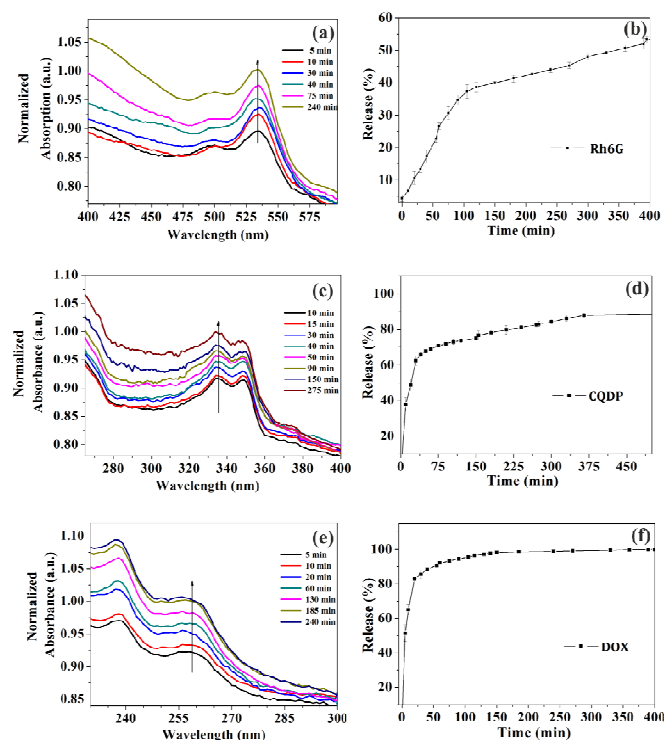


Figure 7: UV-Vis spectra for time dependent release of (a) Rh6G, (c) CQDP and (d) DOX, obtained from formulated SiO₂ hollow nanocapsules. Release kinetics for respective molecules represented in (b), (d) and (f), respectively.

To prove the concept of using our nanocapsules for drug delivery and biomedical applications (*e.g.*, bioimaging, cancer therapy and nano formulation of antimalarial drugs), we have conducted a series of experiments systematically. First, we have checked the loading efficiency of Rh6G (a small fluorescent molecule), DOX (an anticancer drug) and CQDP (an anti-malaria drug) inside the hollow nanocapsules independently and found that these nanocapsules are capable to load fluorescent dye and drug molecules into them. To verify this activity, 1000 μg of our hollow SiO₂ nanocapsules were incubated in the dye/drug solution in dark (at 25°C, pH~7.2, in PBS). And further the *in vitro* release kinetics of the dye/drugs have been studied for all the nanoformulated samples at 37°C using UV-Vis spectroscopy.

The efficiency of release was calculated considering the highest absorption peak position λ_{max} (for Rh6G, CQDP, and DOX are 534 nm, 348 nm, 258 nm, respectively) (Figure 7). From the absorption spectra it is found that the total amount of Rh6G has released into PBS from 1000 μg of Rh6G loaded nanocapsules is ~ 38 μg , from 1000 μg of CQDP loaded nanocapsules is ~ 28.8 μg , and from 1000 μg of DOX loaded nanocapsules is ~ 72 μg . These substantial sustained release data of the dye/drugs represent that the nanocapsules are hollow and porous in nature. Due to the hollow structures these nanocapsules are capable of loading dye/drugs and thus the central cavity acts as a reservoir for the dye/drug. Additionally, the pores on the shells of these nanocapsules act as channel to

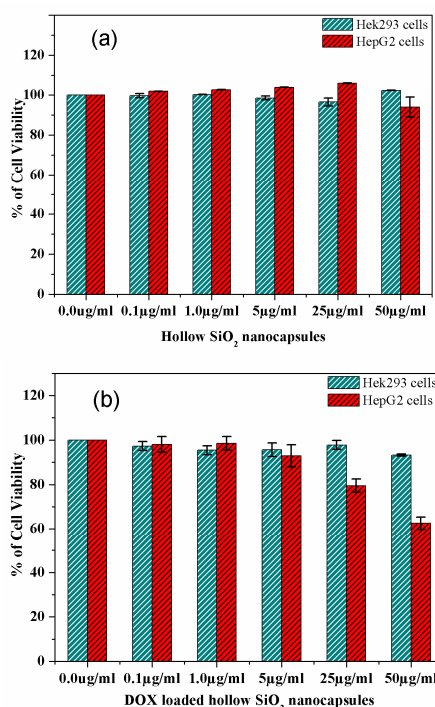


Figure 8 Cytotoxicity assay of Hek293(Human embryonic kidney cell line) and HepG2 cells (Human carcinoma cell line) (a) with mesoporous SiO₂ nanocapsules free from drugs and (b) nano formulated hollow SiO₂ nanocapsules (DOX loaded hollow SiO₂ nanocapsules) with different doses.

release the dye/drug from the central cavity of the nanocapsules through the diffusion process. Therefore, these results are very influencing in future therapeutic applications of the CPMV templated hollow SiO₂ nanocapsules which actually is a bio-silica and free from surfactant related issues because we have not used any surfactant during its synthesis other than CPMV, APTS and TEOS.

In vitro cell viability studies of novel mesoporous hollow silica nanocapsules and nano formulated DOX-loaded hollow silica nanocapsules was carried out using MTT assay against HepG2 cells and Hek293 cells taking 5×10^3 number of cells per well. It is worth mentioning that the cell viability in the hollow nanocapsules/fibers mediated transfection is under the synergetic influence of the cytotoxicity caused by the transfection reagents (nucleic acids) and the surface chemistry of the nanoparticles/fibers system.^[55-56] Similar incident is true for delivery of drugs and the interactions between drug molecules and cells will be different due to the differences in the surface chemistry. To study the cell viability on the unloaded hollow SiO₂ nanocapsules and DOX loaded hollow silica nanocapsules (nanoformulated capsules) an MTT assay was performed at 24 hrs post interaction with both types of samples (DOX loaded and unloaded) (Figure 8) with HepG2 and Hek293 in varying the nanocapsules concentrations of 0.1, 1, 10, 25 and 50 $\mu\text{g}/\text{ml}$ in PBS (pH 7.2) at 37°C. Compared to the control sample the cell viability maximum observed is 95% irrespective to the cell lines (HepG2 or Hek293) which is

similar to the cell viability observed for RAW 264.7 cell lines. Whereas, the cytotoxicity effects of the DOX-loaded hollow SiO₂ nanocapsules on human carcinoma HepG2 cell lines is observed to be 98 (±1) %, 92 (±3) %, 78 (±4.3) % and 62 (±4.2) % at concentration of DOX loaded silica nanocapsules 1, 5, 25 and 50 µg/ml in PBS used, respectively. Where, the actual DOX dosages used are 0.062 µg, 0.36 µg, 1.80 µg and 3.60 µg, respectively which are calculated based on the release kinetics (Figure 7). Hence, with increase in the amount of dosages the human carcinoma cell survival is increasing in a control manner which is actually our intention to achieve and with this respect our nanoformulated medicine is effective. Further we have calculated the IC₅₀ for nano-formulated DOX with our nanocapsules on the HepG2 cell lines and the value obtained to be 8.3 (±0.25) µM, whereas IC₅₀ for free DOX on HepG2 is found to be 4.5 (±0.15) µM. In earlier study we measured the IC₅₀ for the pure free DOX in leukemia cancer cells (K562)^[51(b)] and found to be 1.10 µM which was very close to the IC₅₀ reported value for the HeLa cells.^[57-58] In our earlier work the IC₅₀ for {(ZnO)_n⁶⁺-(DOX)_m} (a nano-formulated complex of DOX with self-assembled ZnO 'dandelions' capsules) in leukemia cancer cells K562 has been measured and the value obtained is 3.32 (±0.12) µM.^[51(b)] Further, IC₅₀ for free DOX on HepG2 reported in literature is 4.6 µM (±0.23)^[59] which is matching well with our present result with free DOX (IC₅₀ = 4.5 ±0.21 µM). Whereas, the obtained higher value of IC₅₀ (8.3 ±0.25 µM) for nano-formulated DOX with our mesoporous hollow bio SiO₂ on the HepG2 cell lines is very interesting. This high value of IC₅₀ for HepG2 cell lines obtained is attributed to the (i) high stability of DOX inside the hollow cavity and mesoporous shell of the novel SiO₂ nanocapsules, (ii) regulated sustained release of DOX from the mesopores hollow cavity of nanocapsules due to the electrostatic interactions between -NH₂ and oxygen containing electron reached functional groups (-OH, -O-, -CO- etc.) of DOX,^[51(b)] and (iii) due to the slow and low decomposition of DOX molecules released from the nanocapsules since they are very much protected inside the pores and hollow cavity capsules. To check the cell inhibition efficiency of our nano-formulation on noncancerous cells similar experiments were performed with a Hek293 and found that the inhibition effect is very less (2 % with 50 µg/ml formulated nanocapsules). Therefore, our bio SiO₂ nanocapsules synthesized with CPMV is an effective cargo in nano formulating with DOX and the resultant nanoformulation is very promising in killing the cancer specific cells.

Conclusions

Herein this work a facile strategy has been developed to design idiosyncratic bio-safe of amine functionalized hollow mesoporous SiO₂ nanocapsules using unmodified CPMV. To achieve the hollow mesoporous bio-SiO₂ we have used the unmodified CPMV, which is very much harmless in human health compared to the various other plant virus reported (e.g., Brome mosaic virus,^[32] Tobacco mosaic virus,^[33] Cow pea chlorotic mottle virus,^[60-61] Tomato bushy shunt virus^[62] etc.)

since the present synthesis approach is surfactant free. The new amorphous hollow SiO₂ mesoporous nanocapsules are biocompatible and exhibit an excellent performance in loading and release of the fluorescent molecules (Rh6G) for bioimaging, antimalarial drugs (CQDP) and anticancer drugs (DOX). The biomedical applications of hollow SiO₂ nanocapsules have been studied *in vitro* wherein RAW 264.7, HepG2 and Hek293 cell lines have been used. Cytotoxicity assays have addressed the biosafety of the synthesized hollow SiO₂ nanocapsules. The biocompatibility of these hollow SiO₂ nanocapsules can play a significant role as a delivering agent in the field of clinical biotechnology. Finally *in vitro* cell viability studies of novel mesoporous hollow silica nanocapsules and nano formulated DOX-loaded hollow silica nanocapsules were carried out using MTT assay against HepG2 which is a Human carcinoma cell lines and Hek293 which is a Human embryonic kidney cell lines and found that our bio SiO₂ nanocapsules synthesized in presence of CPMV is effective in nano formulating with DOX and the resultant nanoformulation is very promising in killing the cancer specific cells. However, understanding the interactions between the hollow mesoporous bio-SiO₂ nanocapsules synthesized in presence of CPMV designed for carrying the medicines with living cells are very important to enrich the effectiveness in therapeutic applications.

Acknowledgements

This work is supported by the Department of Science and Technology Fast-Track Grant for Young Scientist (Ref: SR/FTP/ETA-0079/2011). School of Life Sciences, University of Hyderabad for supporting us to do Biological Work and Dr. Debaprasad Shee, IIT Hyderabad for BET experiments.

Notes and references

^a School of Engineering Sciences and Technology, University of Hyderabad.

Electronic Supplementary Information (ESI) available: [TEM and SEM images of control SiO₂ nanocapsules (without CPMV), TEM images of CPMV, AFM images of CPMV, TEM images of SiO₂ with CPMV at different ratios of APTES: TEOS, XRD, DLS and SAED pattern of hollow SiO₂ nanocapsules]. See DOI: 10.1039/b000000x/

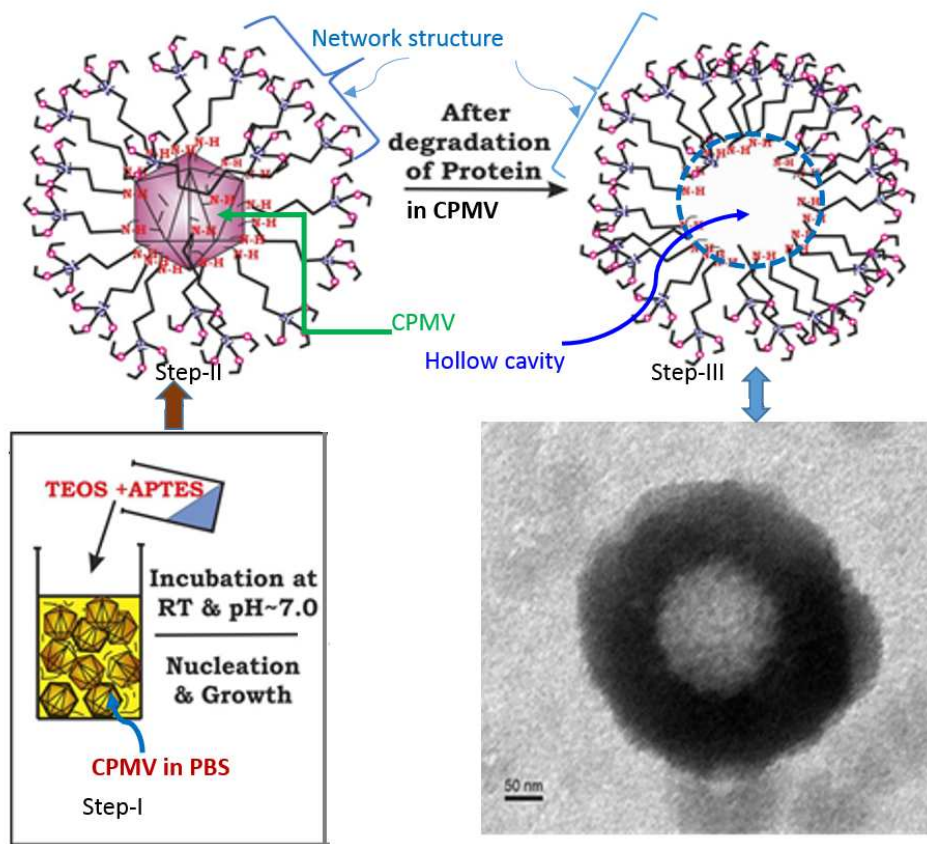
References

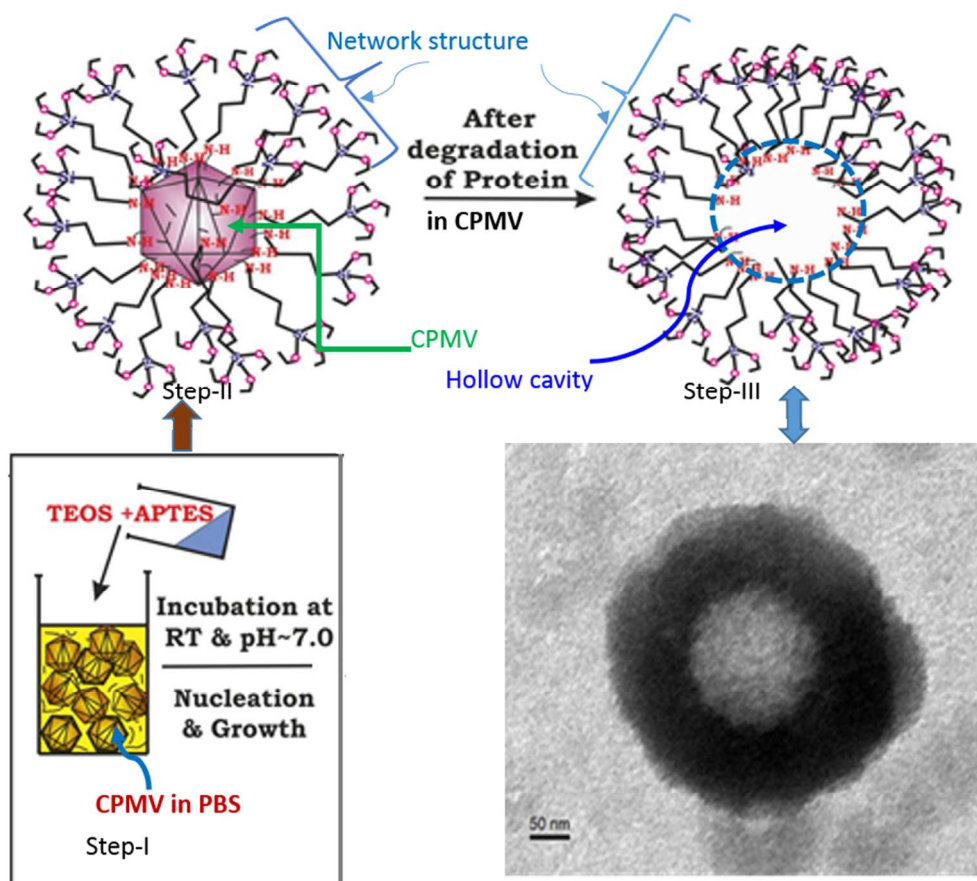
1. J. M. Buriak, *Science*, 2004, **304**, 692–693.
2. Y. Yin, R. M. Rioux, C. K. Erdonmez, S. Hughes, G. a Somorjai, and a P. Alivisatos, *Science*, 2004, **304**, 711–714.
3. C. Lin, W. Zhu, H. Yang, Q. An, C. Tao, W. Li, J. Cui, Z. Li, and G. Li, *Angew. Chem. Int. Ed. Engl.*, 2011, **50**, 4947–4951.
4. S. Tang, X. Huang, X. Chen, and N. Zheng, *Adv. Funct. Mater.*, 2010, **20**, 2442–2447.
5. Y.-L. Luo, Y.-S. Shiao, and Y.-F. Huang, *ACS Nano*, 2011, **5**, 7796–7804.
6. P. Paik and Y. Zhang, *Nanoscale*, 2011, **3**, 2215–2219.
7. E. Morin, M. Nothisen, A. Wagner, and J.-S. Remy, *Bioconjugate Chem.*, 2011, **22**, 1916–1923.
8. S. Hyuk Im, U. Jeong, and Y. Xia, *Nat. Mater.*, 2005, **4**, 671–675.

9. H. Sami, A. K. Maparu, A. Kumar, and S. Sivakumar, *PLoS One*, 2012, **7**, 1–12.
10. B. Li, X. Yang, L. Xia, M. I. Majeed, and B. Tan, *Sci. Rep.*, 2013, **3**, 1–6.
11. *U.S. Patent.*, WO 2013112215 A1, 2013.
12. Y. Tao, J. Han, and H. Dou, *J. Mater. Chem.*, 2012, **22**, 11808–11815.
13. W. Cai, T. Gao, H. Hong, and J. Sun, *Nanotechnol. Sci. Appl.*, 2008, **2008**, 17–32.
14. V. Voliani, F. Ricci, G. Signore, R. Nifosi, S. Luin, F. Beltram, and R. Nifosi, *Recent Pat. nanomedicine*, 2012, **2**, 34–44.
15. S. Pattanayak, A. Priyam, and P. Paik, *Dalton Trans.*, 2013, **42**, 10597–10607.
16. D. A. Norris, N. Puri, and P. J. Sinko, *Adv. Drug Deliv. Rev.*, 1998, **34**, 135–154.
17. K. E. Fischer, B. J. Alemán, S. L. Tao, R. Hugh Daniels, E. M. Li, M. D. Büniger, G. Nagaraj, P. Singh, A. Zettl, and T. A. Desai, *Nano Lett.*, 2009, **9**, 716–720.
18. Y. Chen, H. Chen, D. Zeng, Y. Tian, F. Chen, J. Feng, and J. Shi, *ACS Nano*, 2010, **4**, 6001–6013.
19. Y. Chen, H. Chen, L. Guo, Q. He, F. Chen, J. Zhou, J. Feng, and J. Shi, *ACS Nano*, 2010, **4**, 529–539.
20. S. Rimmer, S. Carter, R. Rutkaite, J. W. Haycock, and L. Swanson, *Soft Matter*, 2007, **3**, 971–973.
21. C. L. McCormick, B. S. Sumerlin, B. S. Lokitz, and J. E. Stempka, *Soft Matter*, 2008, **4**, 1760.
22. H. Nishino, C.-S. Huang, and K. J. Shea, *Angew. Chem. Int. Ed. Engl.*, 2006, **45**, 2392–2396.
23. N. A. O'Connor, D. A. Paisner, D. Huryn, and K. J. Shea, *J. Am. Chem. Soc.*, 2007, **129**, 1680–1689.
24. G. Vlatakis, L. I. Andersson, R. Müller, and K. Mosbach, *Nature*, 1993, **361**, 645–647.
25. K. A. Whitehead, R. Langer, and D. G. Anderson, *Nat. Rev. Drug Discov.*, 2009, **8**, 129–138.
26. Y. Chen, H. Chen, and J. Shi, *Adv. Mater.*, 2013, **25**, 3144–76.
27. J. Liu, Q. Yang, L. Zhang, H. Yang, J. Gao, and C. Li, *Chem. Mater.*, 2008, **20**, 4268–4275.
28. M. Mandal and M. Kruk, *Chem. Mater.*, 2012, **24**, 123–132.
29. W. Stober and A. Fink, *J. Colloid Interface Sci.*, 1968, **26**, 62–69.
30. J.-T. Wang, H. Wang, X.-M. Ou, C.-S. Lee, and X.-H. Zhang, *Langmuir*, 2011, **27**, 7996–7999.
31. T. Shiomi, T. Tsunoda, A. Kawai, F. Mizukami, and K. Sakaguchi, *Chem. Commun. (Camb.)*, 2007, 4404–4406.
32. J.-W. Kim, A. S. Utada, A. Fernández-Nieves, Z. Hu, and D. a Weitz, *Angew. Chem. Int. Ed. Engl.*, 2007, **46**, 1819–1822.
33. P. Yang, S. Gai, and J. Lin, *Chem. Soc. Rev.*, 2012, **41**, 3679–3698.
34. Q. Wang, T. Lin, J. E. Johnson, and M. G. Finn, *Chem. Biol.*, 2002, **9**, 813–819.
35. X. Huang, B. D. Stein, H. Cheng, A. Malyutin, I. B. Tsvetkova, D. V Baxter, N. B. Remmes, J. Verchot, C. Kao, L. M. Bronstein, and B. Dragnea, *ACS Nano*, 2011, **5**, 4037–4045.
36. A. a Khan, E. K. Fox, M. L. Górzny, E. Nikulina, D. F. Brougham, C. Wege, and A. M. Bittner, *Langmuir*, 2013, **29**, 2094–2098.
37. I. J. Minten, Y. Ma, M. A. Hempenius, G. J. Vancso, R. J. M. Nolte, and J. J. L. M. Cornelissen, *Org. Biomol. Chem.*, 2009, **7**, 4685–4688.
38. S. N. Shah, N. F. Steinmetz, A. A. Aljabali, G. P. Lomonosoff, and D. J. Evans, *Dalton Trans*, 2009, 8479–8480.
39. N. F. Steinmetz, S. N. Shah, J. E. Barclay, G. Rallapalli, G. P. Lomonosoff, and D. J. Evans, *Small*, 2009, **5**, 813–816.
40. E. Royston, S.-Y. Lee, J. N. Culver, and M. T. Harris, *J. Colloid Interface Sci.*, 2006, **298**, 706–712.
41. A. a Khan, E. K. Fox, M. L. Górzny, E. Nikulina, D. F. Brougham, C. Wege, and A. M. Bittner, *Langmuir*, 2013, **29**, 2094–2098.
42. A. K. Manocchi, S. Seifert, B. Lee, and H. Yi, *Langmuir*, 2011, **27**, 7052–7058.
43. J. C. Zhou, C. M. Soto, M.-S. Chen, M. a Bruckman, M. H. Moore, E. Barry, B. R. Ratna, P. E. Pehrsson, B. R. Spies, and T. S. Confer, *J. Nanobiotechnology*, 2012, **10**, 1–12.
44. X. Chen, K. Gerasopoulos, J. Guo, A. Brown, C. Wang, R. Ghodssi, and J. N. Culver, *ACS Nano*, 2010, **4**, 5366–5372.
45. J. E. Johnson and J. A. Speir, *J. Mol. Biol.*, 1997, **269**, 665–675.
46. N. F. Steinmetz, G. P. Lomonosoff, and D. J. Evans, *Langmuir*, 2006, **22**, 3488–3490.
47. Q. Wang, E. Kaltgrad, T. Lin, J. E. Johnson, and M. G. Finn, *Chem. Biol.*, 2002, **9**, 805–811.
48. J. Wellink, *Methods Mol. Biol.*, 1998, **81**, 205–209.
49. J. M. White and J. E. Johnson, *Virology*, 1980, **101**, 319–324.
50. J. E. Johnson and C. Hollingshead, *J. Ultrastruct. Res.*, 1981, **74**, 223–231.
51. (a) V. B. Kumar, M. Annamandeni, M. D. Prashad, K. M. Arunasree, Y. Mastai, A. Gedanken, and P. Paik, *J. Nanoparticle Res.*, 2013, **15**, 1904, 1–13. (b) V. B. Kumar, K. Kumar, A. Gedanken, and P. Paik, *J. Mater. Chem. B*, 2014, **2**, 3956–3964.
52. A. a. Aljabali, J. E. Barclay, O. Cespedes, A. Rashid, S. S. Staniland, G. P. Lomonosoff, and D. J. Evans, *Adv. Funct. Mater.*, 2011, **21**, 4137–4142.
53. P. Paik, A. Gedanken, and Y. Mastai, *ACS Appl. Mater. Interfaces*, 2009, **1**, 1834–1842.
54. H. Hu, H. Zhou, J. Liang, L. An, A. Dai, X. Li, H. Yang, S. Yang, and H. Wu, *J. Colloid Interface Sci.*, 2011, **358**, 392–398.
55. P. Rujitanaroj, Y.-C. Wang, J. Wang, and S. Y. Chew, *Biomaterials*, 2011, **32**, 5915–5923.
56. H. Cao, X. Jiang, C. Chai, and S. Y. Chew, *J. Control. Release*, 2010, **144**, 203–212.
57. K. C. Barick, S. Nigam, and D. Bahadur, *J. Mater. Chem.*, 2010, **20**, 6446–6452.
58. D. Y. Lu, M. Huang, C. H. Xu, W. Y. Yang, C. X. Hu, L. P. Lin, L. J. Tong, M. H. Li, W. Lu, X. W. Zhang, and J. Ding, *BMC Pharmacol.*, 2005, **5**, 11.
59. M. Al-Qubaisi, R. Rozita, S.-K. Yeap, A.-R. Omar, A.-M. Ali, and N. B. Alitheen, *Molecules*, 2011, **16**, 2944–2959.
60. F. D. Sikkema, M. Comellas-Aragonès, R. G. Fokkink, B. J. M. Verduin, J. J. L. M. Cornelissen, and R. J. M. Nolte, *Org. Biomol. Chem.*, 2007, **5**, 54–57.
61. M. Comellas-Aragonès, A. de la Escosura, a T. J. Dirks, A. van der Ham, A. Fusté-Cuñé, J. J. L. M. Cornelissen, and R. J. M. Nolte, *Biomacromolecules*, 2009, **10**, 3141–3147.
62. J. K. Pokorski and N. F. Steinmetz, *Mol. Pharm.*, 2010, **8**, 29–43.

ARTICLE

Graphical Abstract: Synthesis of CPMV- Hollow silica nanocapsules and its used in Nanomedicine.





243x221mm (96 x 96 DPI)